Seed induced growth of binary Ag/Au nanostructures on a graphite surface

N. Lidgi-Guigui[a, *], P. Mulheran[b] and R. E. Palmer[a]

[a]Nanoscale Physics Research Laboratory, School of Physics and Astronomy, University of

Birmingham, Birmingham B15 2TT, United Kingdom

[b]Department of Physics, The University of Reading, Whiteknights, Reading RG6 6AF, United

Kingdom

The growth of Ag on a graphite surface decorated by size selected Au "seed" nanoclusters is investigated. Compared with the behaviour on bare graphite, the deposition of the Au clusters decreases the lateral diffusion of Ag atoms and enables the growth of Ag/Au nanostructures based on the initial Au clusters. Depending on the Au cluster shape, which can be tuned by the cluster deposition energy, Ag deposition either leads to two monolayer high platelets or 3D nanoclusters. This cluster seeding technique shows potential for the rapid production of binary model catalysts, biochips and optical films.

* Current address

Laboratoire d'Electronique Moléculaire,

SPEC / IRAMIS bat 125

CEA, Saclay

91125 Saclay Cedex, France

Noble metal nanostructures are the focus of growing interest for several reasons. The main one is that these **new** objects combine the physics emerging at the nanoscale with the intrinsically high stability of their constituent element. This explains why the use of such nanostructures is reported in an increasing number of publications centred on very different topics, such as biomedical imaging[1 2], surface enhanced Raman scattering[3 4 5] or catalysis[6 7 8]. Among noble metal nanostructures, nanoparticles made from Au and Ag are of particular interest since their localized surface plasmon resonance peaks lie in the visible or near UV regions. Combinations of these two elements show even more diverse properties. As one example, bimetallic particles have proved to be more efficient in catalysis than their individual elements[9 10 11 12]. Bimetallic nanoclusters can be synthesized by a variety of chemical methods[13 14 15]; however, some physical approaches also exist, mainly laser ablation from an alloy target[16 17]. In this latter approach, the clusters generated are most often nanoalloys. In the chemical approach, the concept of seeding is often exploited[18 19 20], e.g., Au colloids are synthesized in solution with a shell of ligand molecules having affinity to Ag^+; after a final reduction step, the molecular shell is removed leaving a $Au_{core}Ag_{shell}$ structure. To our knowledge. There is a recent report of seeding in the context of a physical method[21], but these authors did not employ size selected clusters nor investigate the underlying growth mechanisms.

Here we investigate the evaporation of Ag atoms on a graphite surface pre-decorated by the deposition of size selected Au nanoclusters, with the aim of growing bimetallic nanostructures on the surface. The model graphite (Highly Oriented Pyrolytic Graphite, HOPG) surface is chosen because the defect density is very low and so the probability of growing Ag-only clusters by nucleation at natural defects is reduced to a minimum.

The size-selected Au clusters were produced with a radio-frequency magnetron sputtering, gas condensation cluster beam source described previously[22 23]. The clusters were mass-selected by a

novel lateral Time-of-Flight mass selector [24] operated with a resolution of ±2% independent of the cluster mass. Two sizes of clusters were used, Au_{250} and Au_{2000} (i.e., clusters consisting respectively of 250 and 2000 atoms of Au). They were deposited on freshly cleaved graphite samples in one of two ways. The first consists of depositing Au clusters at high energy (typically 20eV per atom) in order to self-pin the clusters on the surface[25][26][27][28]: the cluster impact on the substrate displaces a surface carbon atom from the graphite lattice, and the Au cluster is then trapped by this defect. The maximum available energy in our set-up is 5keV per cluster, so as a consequence Au_{250} is one of the biggest Au clusters that can be efficiently self-pinned. The second technique is soft-landing the clusters onto an assembly of defects made by *in-situ* sputtering of the graphite surface with an Ar^+ beam at 500eV[29]. In both cases, immediately after the Au cluster deposition the nanostructured graphite samples were transferred into a home made thermal evaporator[30] where Ag was evaporated. The evaporation rate was calibrated by measuring the thickness of a Ag layer deposited on glass and was about 10^{12} atoms per second.

The characterization of the samples was carried out mainly using an Atomic Force Microscope (AFM) (Digital Instruments Dimension 3100) equipped with a Nanoscope IIIa controller. The tips used were standard oxide-sharpened silicon nitride tips with a spring constant of 0.6 N/m. However, the Au_{250} clusters self-pinned on graphite were below the resolution limits of the AFM. So the corresponding Scanning Tunneling Microscope (STM) head was employed instead (also in ambient conditions). Typical imaging parameters were a sample bias of +0.4 V and a tunnel current of +0.4 nA. Mechanically cut PtIr tips were employed. For both the AFM and STM measurements, the maximum cluster height was measured, after height calibration on graphite steps, using the grain analysis module of the SPIP[31] image processing program.

Fig. 1(a) shows a tapping mode AFM scan of Ag (one 0.01 monolayers) evaporated on a sub-monolayer film of immobilized Au_{2000} clusters (mean spacing 162 nm). The behaviour is different

from the case when Ag is evaporated in the absence of Au clusters quite different features are observed,[32] because the lateral Ag diffusion length is reduced by the clusters. Small Ag clusters formed between the Au clusters by homogeneous nucleation of a few Ag atoms on graphite[27] would lie well below the AFM resolution, so could not appear in fig. 1(a) To minimize the probability of Ag cluster growth on isolated Ar^+ defects, we have deposited as many Au clusters as Ar^+ defects. The height distribution of Au_{2000} soft-landed on Ar^+ sputtered graphite before and after Ag evaporation, as shown in fig. 1(b), presents a mean height shifted upwards by almost 1nm after Ag evaporation. No peak is found at the Au_{2000} mean height after Ag evaporation. It therefore seems that Ag either forms a shell around the Au clusters or alloys with it to generate the larger particles observed. Thus cluster-seeded growth of binary metal nanoparticles on the surface is established.

To understand the nature of the clusters observed after Ag evaporation we have performed simulations based on a point-island model of cluster nucleation and growth during vapour deposition[33] [34]; results are shown in fig. 2. Ag growth only on the Au cluster seeds creates a distribution of cluster masses centred on the average value of 5000 atoms. Growth without seeds produces a broader, asymmetric distribution of sizes, centred on the average size of 3000 atoms, but which extends from zero to about 6000 atoms[35]. The case of growth on the seeds alongside an equivalent number of nucleation events produces a bi-modal size distribution. If we assume the clusters are growing in a 3D fashion, then the cluster height correlates with the cube-root of mass, and a bi-modal distribution of heights would be observed experimentally if there were significant nucleation of Ag-only clusters - but this is not the case. Alternatively, we might suppose that the clusters grow to a constant height, once they are large enough. In this case, we need to consider how many nucleated clusters would be observed in the AFM. As can be seen from fig. 2, many of the nucleated clusters in the simulation are of comparable size to the initial Au_{2000} seeds, and so would appear in the data. In this case, the density of clusters observed after Ag deposition would

be significantly greater than that found before, and this is also not the case. We can conclude that the majority of the deposited Ag is being captured by the Au seeds.

To extend the experimental investigation further, the same experiment was performed using Au_{250} clusters instead of Au_{2000}. The results are illustrated by the XXX image??... shown in fig. 3 [need to say if AFM or STM here]. As for Au_{2000}, a shift of 1nm towards larger sizes is observed for Au_{250} after Ag evaporation. The growth of Ag on Au seeds is thus a general feature independent of cluster seed size. Similar effects as those obtained with Au_{2000} cluster are observed. While as noted Au_{250} clusters soft landed on Ar^+ defects lie below the AFM resolution, the clusters become clearly visible after Ag evaporation, a comparison between STM and AFM data (before and after Ag evaporation) shows that the size shift is again about 1nm towards the larger sizes after Ag deposition. Ag growth on graphite supported Au clusters is thus taking place in the same way on Au_{2000} and Au_{250}, it is not critically governed by a cluster size effect, for example.

- should not start new para here -

As previously mentioned, Au_{250} can either be soft-landed on Ar^+ sputtered graphite or self-pinned at sufficiently high cluster impact energy (which also leads to flattening of the clusters). The height of Ag clusters grown on both kinds of samples is shown in fig. 3(b). Three monolayer high Ag platelets (i.e. 0.4 nm) are observed when Ag is deposited onto self-pinned Au clusters. This contrasts with the, on average, 1.5nm high clusters found when Ag is evaporated on the graphite surface decorated with Au clusters soft-landed on Ar^+ defects. Evidently, the atomic structure of the Au seed particles regulates the morphology of the binary structure generated from it. It seems likely that this behaviour reflects the different facets and edge atoms presented by the two different cluster shapes. Add the references from the next para then you can delete it as you suggested.

The growth of Ag on Au nanoparticles has previously been described by [18] in the context of chemical synthesis and the presence stabilising molecules. Anisotropic growth was observed and assigned to faster growth of {100} side facets than {110} facets. We believe that similar physics can explain the strong influence the cluster shape on the resulting binary nanoparticle morphology. We expect the soft-landed Au_{250} clusters (pinned at Ar^+ defects) to show a 3D morphology[36] analogous to the gas phase cluster. In this case we envisage the binary particle growing in all three dimensions since the lattice constants of Ag and Au are very similar (within 0.3%), as reflected in the increase in height (~ 1nm) of both the Au_{250} and Au_{2000} clusters when Ag is evaporated. In the case of the self-pinned Au_{250} clusters, the clusters are deformed on landing into a quasi-two-dimensional morphology one or two monolayer in height[26][37]. Assuming the presence of low coordinated Au atoms at the edges of these platelets[38][39], we then envisage selective attachment of Ag atoms to the cluster circumference, leading to lateral growth of the (now binary) platelets. This explains the limited height of the binary particles generated by Ag addition to the self-pinned Au_{250} clusters. Assuming you will now delete this para

In summary, the growth of Ag/Au binary nanoparticles on graphite by evaporation of Ag atoms on size selected Au clusters (seeds) has been demonstrated through a combination of experiment and computer simulation.. Moreover, our results show that the morphology of the nanostructures produced is strongly influenced by the shape of the seed clusters. The results suggest several avenues for additional experimental investigations of these novel systems, e.g., atom-resolved electron microscopy studies[28]. From an applied perspective, the regulation by size-selected cluster seeds of the size and morphology of binary nanoparticles in which most of the atoms are simply deposited by evaporation (a cheap and efficient method) suggests a practical route to the generation of nanostructured functional films.
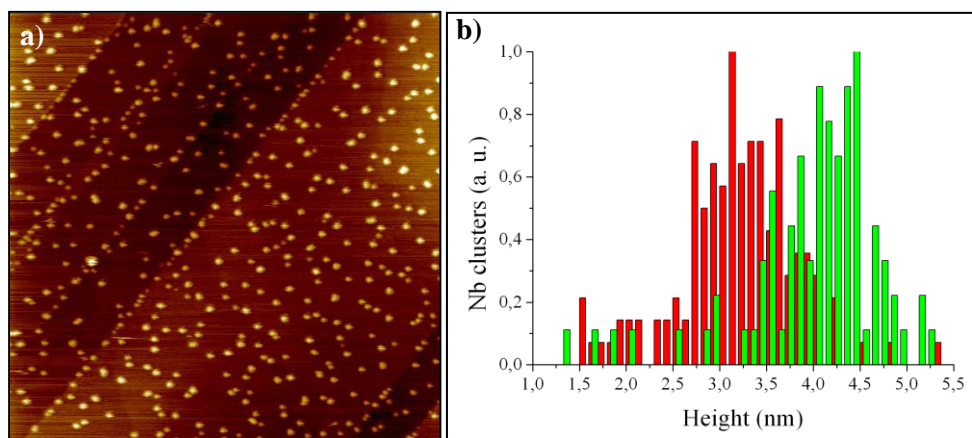
FIG. 1: (a) AFM image of Au$_{2000}$ clusters soft-landed on Ar$^+$ sputtered graphite after silver evaporation (3μm x 3μm). (b) Height distribution of the clusters before (red) and after (green, as (a)) one 1/100 silver monolayer evaporation.
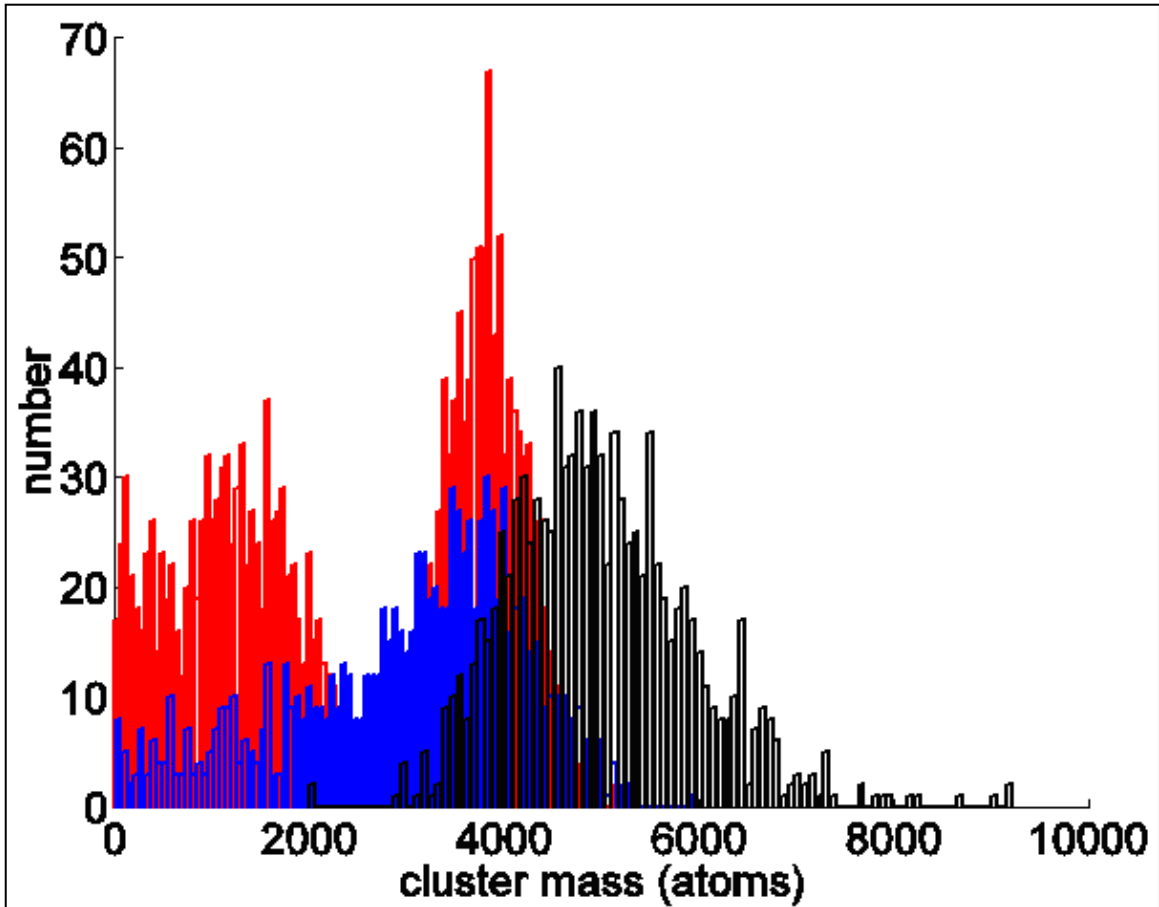
FIG. 2: Cluster mass distributions from three simulations: growth only on the seed particles (black); nucleation and growth without seeds (blue); and growth on seeds plus significant nucleation (red).
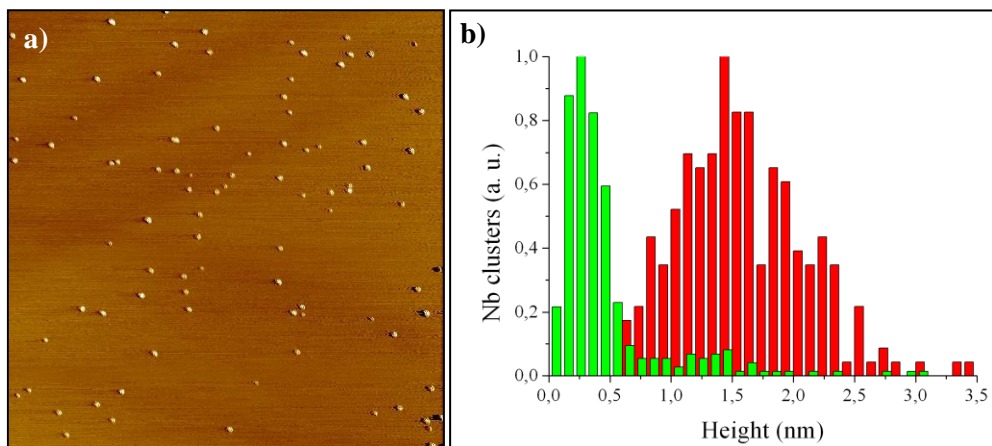
FIG 3: (a) STM image of Au $_{250}$ clusters self-pinned on graphite. (b) Height distribution of self-pinned Au$_{250}$ clusters, as (a), after Ag evaporation (green); height distribution of Au250 clusters soft-landed on Ar$^+$ sputtered graphite after Ag evaporation (red).

[1] B. Dubertret, P. Skourdis, D. J. Norris, V. Noireaux, A. H. Brivanlou, A. Libchaber, Science **29**, 161 (2002).

[2] E. Klarreich, Nature **413**, 450 (2001).

[3] T. Pham, J. B. Jackson, N. J. Halas, T. R. Lee, Langmuir **18**, 4915 (2002).

[4] M. L. Zhang, C. Q. Yi, X. Fan, K. Q. Peng, N. B. Wong, M. S. Yang, R. Q. Zhang, S. T. Lee, App. Phys. Lett. **92**, 043116 (2008).

[5] J. B. Jackson, S. L. Westcott, L. R. Hirsch, J. L. West, N. J. Halas, App. Phys. Lett. **82**, 257 (2003).

[6] J. H. Sinfelt, Surface Science **500**, 923 (2002).

[7] L. N. Lewis, Chem. Rev. **93**, 2693 (1993).

[8] M. C. Daniel, D. Astruc, Chem. Rev. **104**, 293 (2004).

[9] N. Dimitratos, F. Porta, L. Prati, A. Villa, Catal. Lett. 2005, 99, 181 (2005).

[10] M. O. Nutt, K. N. Heck, P. Alvarez, M. S. Wong, Appl. Catal. B **69**, 115 (2006).

[11] A. M. Venezia, V. La Parola, G. Deganello, B. Pawelec, J. L. G. Fierro, J. Catal. **215**, 317 (2003).

[12] E. A. Sales, B. Benhamida, V. Caizergues, J.-P. Lagier, F. Fiévient, F. Bozon-Verduraz, Appl. Catal. A **172**, 273 (1998).

[13] S. W. Han, Y. Kim, K. Kim, J. Colloid Interface Sci. 208, **272** (1998).

[14] H. Hodak, A. Henglein and M. Giersig. J. Phys. Chem. B **104**, 117087 (2000).

[15] J. Zhu, Y.C. Wang and Y.M. Lu. Colloids Surf. A **232**, 155 (2004).

[16] I. Lee, S. Woo Han, K. Kim, Chem. Comm.**18**, 1782 (2001).

[17] L. Favre, V. Dupuis, E. Bernstein, P. Mélinon, and A. Pérez, S. Stanescu T. Epicier J.-P. Simon D. Babonneau, Phys. Rev. B **74**, 014439 (2006).

[18] S. Prathap Chandran J. Ghatak, P.V. Satyam, Murali Sastry, J. of Colloid and Interface Science **312**, 498 (2007).

[19] P. Selvakannan, A. Swami, D. Srisathiyanarayanan, P. S. Shirude, R. Pasricha, A. B. Mandale, M. Sastry, Langmuir 20, 7825 (2004).

[20] Y. Xiang, X. Wu, D. Liu, Z. Li, W. Chu, L. Feng, K. Zhang, W. Zhou, S. Xie, Langmuir **24**, 3465 (2008).

[21] M. Cazayous, C. Langlois, T. Oikawa, C. Ricolleau, A. Sacuto, Phys. Rev. B **73**, 113402 (2006).

[22] I. M. Goldby, B. von Issendorff, L. Kuipers, R. E. Palmer, Rev. Sci Instrum. **68**, 3327 (1997).

[23] S. Pratontep, S. J. Caroll, C. Xirouchaki, M. Streun, R. E. Palmer, Rev. Sci. Inst. **76**, 045103 (2005).

[24] B. von Issendorff, R. E. Palmer, Rev. Sci. Instrum. **70**, 4497 (1999).

[25] S. J. Carroll, S. Pratontep, M. Streun, R. E. Palmer, S. Hobday, R. Smith, J. Chem. Phys. **113**, 7723 (2000).

[26] M. Di Vece, S. Palomba, R. E. Palmer, Phys. Rev. B. **72**, 073407 (2005).

[27] R. Smith, C. Nock, S. D. Kenny, J. J. Belbruno, M. Di Vece, S. Palomba, R. E. Palmer, Phys. Rev. B **73**, 125429 (2006).

[28] R. E. Palmer, S. Pratontep, H.-G. Boyen, Nautre Mat. **2**, 443 (2003).

[29] F. Claeyssens, S. Pratontep, C. Xirouchaki, R. E. Palmer, Nanotechnology **17**, 805 (2006).

[30] S. J. Park Ph.D. thesis, University of Birmingham (2006).

[31] http://www.imagemet.com/

[32] G. M. Francis, I. M. Goldby, L. Kuipers, B. von Issendorff, R. E. Palmer, J. Chem. Soc. Dalton Trans. **5**, 665 (1996).

[33] M .C. Bartelt, J.W. Evans, Phys. Rev. B **46** ,12675 (1992).

[34] J.A. Venables, Philos. Mag. **27**, 697 (1972).

[35] P.A. Mulheran and J.A. Blackman, Phys. Rev. B 53, 10261 (1996).

[36] Z. Y. Li, N. P. Young, M. Di Vece, S. Palomba, R. E. Palmer, A. L. Bleloch, B. C. Curley, R. L. Johnston, J. Jiang and J. Yuan, Nature **451,** 46 (2007).

[37] S. J. Caroll, P. Weibel, B. von Issendorff, L. Kuiper, R. E. Palmer, J. Phys. Cond. Mat. **8**, L617 (1996).

[38] N. Lopez, J. K. Norskov, J. Am. Chem. Soc. **124**, 11262 (2002).

[39] J. A. van Bokhoven, C. Louis, J. T. Miller, M. Tromp, O. V. Safonova, P. Glatzel, Angew. Chem. Int. Ed. **45**, 4651 (2006).